

Higgs-boson coupling to charginos in the MSSM at linear colliders.

G. Ferrera^{1,2)a)}, B. Mele^{2,1)b)}

1. Università di Roma “La Sapienza”, Rome, Italy 2. INFN, Sezione di Roma, Rome, Italy

Abstract — We discuss the associated production of a light Higgs boson (h) and a light chargino ($\tilde{\chi}_1^\pm$) pair in the process $e^+e^- \rightarrow h \tilde{\chi}_1^+ \tilde{\chi}_1^-$ in the Minimal Supersymmetric Standard Model (MSSM) at linear colliders (LC) with $\sqrt{s} = 500 \text{ GeV}$. This process gives direct informations about Higgs-boson coupling to light charginos which cannot be analyzed in decay processes due to phase-space restriction. We compute total cross sections in the regions of the MSSM parameter space where the process $e^+e^- \rightarrow h \tilde{\chi}_1^+ \tilde{\chi}_1^-$ cannot proceed via on-shell production and subsequent decay of either heavier charginos or pseudoscalar Higgs bosons A . Cross sections up to a few 0.1 fb are allowed, making this process potentially detectable at high-luminosity LC. We also compute analytically the final h momentum distributions in the limit of heavy electron-sneutrino masses, $m_{\tilde{\nu}_e} \gg M_W$.

1 Introduction

In this talk we present the main features of the work discussed more exhaustively in [1]. We know that linear colliders with $\sqrt{s} = 500 \text{ GeV}$ would be a very powerful *precision instrument* for Higgs-boson physics and physics beyond the standard model (SM) that could show up at the LHC. In fact, if supersymmetry (SUSY) exists with partners of known particles with masses not too far from present experimental limits, it will be necessary to study the details of new physics in order to understand which SUSY scenario is effectively realized. Next-generation linear colliders such as TESLA and NLC/JLC [2] would be able to measure (sometimes with excellent precision) a number of crucial parameters (such as masses, couplings and mixing angles), and eventually test the fine structure of a particular SUSY model.

We know that the Higgs couplings to particle are strictly related to the mass of particles. In the case of light particle the Higgs couplings are suppressed (as for the light fermions couplings to the Higgs bosons, where $g_{hff} \sim m_f/v$) and the coupling can generally be determined through the corresponding Higgs decay branching ratio measurement.

On the other hand, the Higgs couplings to vector bosons are unsuppressed and the analysis of the main Higgs-boson production cross section, that occurs through the couplings to vector bosons, can provide a good determination of such couplings.

There are a number of Higgs-boson couplings to quite heavy particles, other than gauge bosons, that can not be investigated through Higgs-boson decay channels due to phase-space restrictions. In this case, the associated production of a Higgs boson and a pair of the heavy particles, when allowed by phase space, can provide an alternative to measure the corresponding coupling, even if some reduction in the rate due to the possible phase-space saturation is expected.

For instance, the SM Higgs-boson *unsuppressed* coupling to the top quark, m_t/v , can be determined at linear colliders with $\sqrt{s} \sim 1 \text{ TeV}$ through the production rates for the Higgs radiated off a top-quark pair in the channel $e^+e^- \rightarrow h t\bar{t}$ [3].

Our purpose is to use the latter strategy in the context of the MSSM, that introduces an entire spectrum of relatively heavy partners, in many cases coupled to Higgs bosons via an unsuppressed coupling constant. A typical example

^{a)}Talk presented by G.Ferrera, e-mail: giancarlo.ferrera@roma1.infn.it

^{b)}e-mail: barbara.mele@roma1.infn.it

is that of the light Higgs-boson coupling to the light top squark $h \tilde{t}_1 \tilde{t}_1^*$, that can be naturally large. The continuum production $e^+e^- \rightarrow h \tilde{t}_1 \tilde{t}_1^*$ has been studied in [4] as a means of determining this coupling (the corresponding channel at hadron colliders has been investigated also in [5]). The Higgs coupling to the τ slepton has been considered in [6].

Here, we discuss the possibility to measure the light Higgs coupling to light charginos $h \tilde{\chi}_1^+ \tilde{\chi}_1^-$ through the Higgs-boson production in association with a chargino pair at linear colliders through the process

$$e^+e^- \rightarrow h \tilde{\chi}_1^+ \tilde{\chi}_1^- . \quad (1)$$

We will not include in our study the case where the considered process proceeds through the on-shell production of either the heavier chargino $\tilde{\chi}_2^-$ or the pseudoscalar Higgs boson A with a subsequent decay $\tilde{\chi}_2^- \rightarrow h \tilde{\chi}_1^-$ and $A \rightarrow \tilde{\chi}_1^+ \tilde{\chi}_1^-$, respectively. We will also assume a large value for the electron sneutrino mass (i.e., $m_{\tilde{\nu}_e} > 1$ TeV). This suppresses the Feynman diagrams with a sneutrino exchange, involving predominantly the gaugino components of the charginos. Note that while *heavy* Higgs bosons couplings to SUSY partners can be mostly explored via Higgs decay rates, the *light* Higgs-boson coupling to light charginos cannot be investigated through Higgs decay channels due to phase-space restrictions. Indeed, in the MSSM m_h is expected to be lighter than about 130 GeV [7], and the present experimental limit on the chargino mass $m_{\tilde{\chi}_1^+} > 103.5$ GeV (or even the milder one $m_{\tilde{\chi}_1^+} > 92.4$ GeV, in case of almost degenerate chargino and lightest neutralino) [8] excludes the decay $h \rightarrow \tilde{\chi}_1^+ \tilde{\chi}_1^-$.

Note that the SM process $e^+e^- \rightarrow HW^+W^-$ (that can be connected by a SuSy transformation to $e^+e^- \rightarrow h \tilde{\chi}_1^+ \tilde{\chi}_1^-$) has a total cross section of about 5.6 fb for $m_H \simeq 120$ GeV, at $\sqrt{s} \simeq 500$ GeV [9].

2 Relevant MSSM Scenarios

In the MSSM, charginos are the mass eigenstates of the mass matrix that mixes charged gauginos and higgsinos (see [10], [1]). At tree level, the mass eigenvalues $m_{\tilde{\chi}_1^+}$ and $m_{\tilde{\chi}_2^+}$ and the mixing angles can be analytically written in terms of the parameters M_2 , μ and $\tan\beta$. The presence of a Higgs boson in the process $e^+e^- \rightarrow h \tilde{\chi}_1^+ \tilde{\chi}_1^-$ requires a further parameter, that can be the pseudoscalar mass m_{A^0} . On the other hand, the inclusion of the main radiative corrections to the Higgs-boson mass and couplings involves all the basic parameters needed for setting the complete mass spectrum of the SuSy partners in the MSSM. We set $m_{A^0} = 500$ GeV, this pushes the pseudoscalar field A^0 beyond the threshold for direct production, thus preventing resonant $A^0 \rightarrow \tilde{\chi}_1^+ \tilde{\chi}_1^-$ contribution to the $h \tilde{\chi}_1^+ \tilde{\chi}_1^-$ final state. At the same time, this choice for m_{A^0} sets a *decoupling-limit* scenario ($m_{A^0} \gg M_Z$).

Present experimental lower limits on m_h [11] in the *decoupling-limit* MSSM are close to the ones derived from the SM Higgs boson direct search (i.e., $m_H > 114.4$ GeV at 95% C.L. [12]).

The corrections to the light Higgs mass and coupling parameter α have been computed according to the code FeynHiggsFast [13], with the following input parameters : $M_{\tilde{t}_{L,R}} = M_{\tilde{b}_{L,R}} = M_{\tilde{g}} = 1$ TeV , $X_t (\equiv A_t - \mu \cot\beta) =$ either 0 or 2 TeV, $A_b = A_t$, $m_t = 175$ GeV, $m_b = 4.5$ GeV, $\mu = 200$ GeV, $M_2 = 400$ GeV, and renormalization scale at m_t , in the most complete version of the code (varying the μ and M_2 parameters would affect the Higgs spectrum and couplings negligibly).

We assumed three different $\tan\beta$ scenarios, and corresponding m_h values for $m_{A^0} = 500$ GeV:

- a)** $\tan\beta = 3$, with *maximal* stop mixing (i.e., $X_t = 2$ TeV), and $m_h = 120.8$ GeV;
- b)** $\tan\beta = 15$, with *no* stop mixing (i.e., $X_t = 0$), and $m_h = 114.3$ GeV;
- c)** $\tan\beta = 30$, with *maximal* stop mixing (i.e., $X_t = 2$ TeV), and $m_h = 132.0$ GeV;

that are allowed by present experimental limits [11]. In this talk we focalize on the scenario **a**).

There are 13 Feynman diagrams involved in the process $e^+e^- \rightarrow h \tilde{\chi}_1^+ \tilde{\chi}_1^-$, 7 with the s -channel Z^0/γ exchange and 6 with the t -channel electron-sneutrino $\tilde{\nu}_e$ exchange. In our cross-section evaluation, we include only the s -channel diagrams reported in Fig. 1, and disregard the 6 diagrams in Fig. 2. In fact the latter are expected to contribute moderately to the cross section in the case $m_{\tilde{\nu}_e} > 1$ TeV, $m_{A^0} = 500$ GeV. We discuss the accuracy of this assumption in [1]. In Fig. 3, we show (in grey), the area in the (μ, M_2) plane that is of relevance for the *non resonant* $e^+e^- \rightarrow h \tilde{\chi}_1^+ \tilde{\chi}_1^-$ process. The solid lines correspond to the threshold energy contour level :

$$\sqrt{s} = 2 m_{\tilde{\chi}_1^+} + m_h, \quad (2)$$

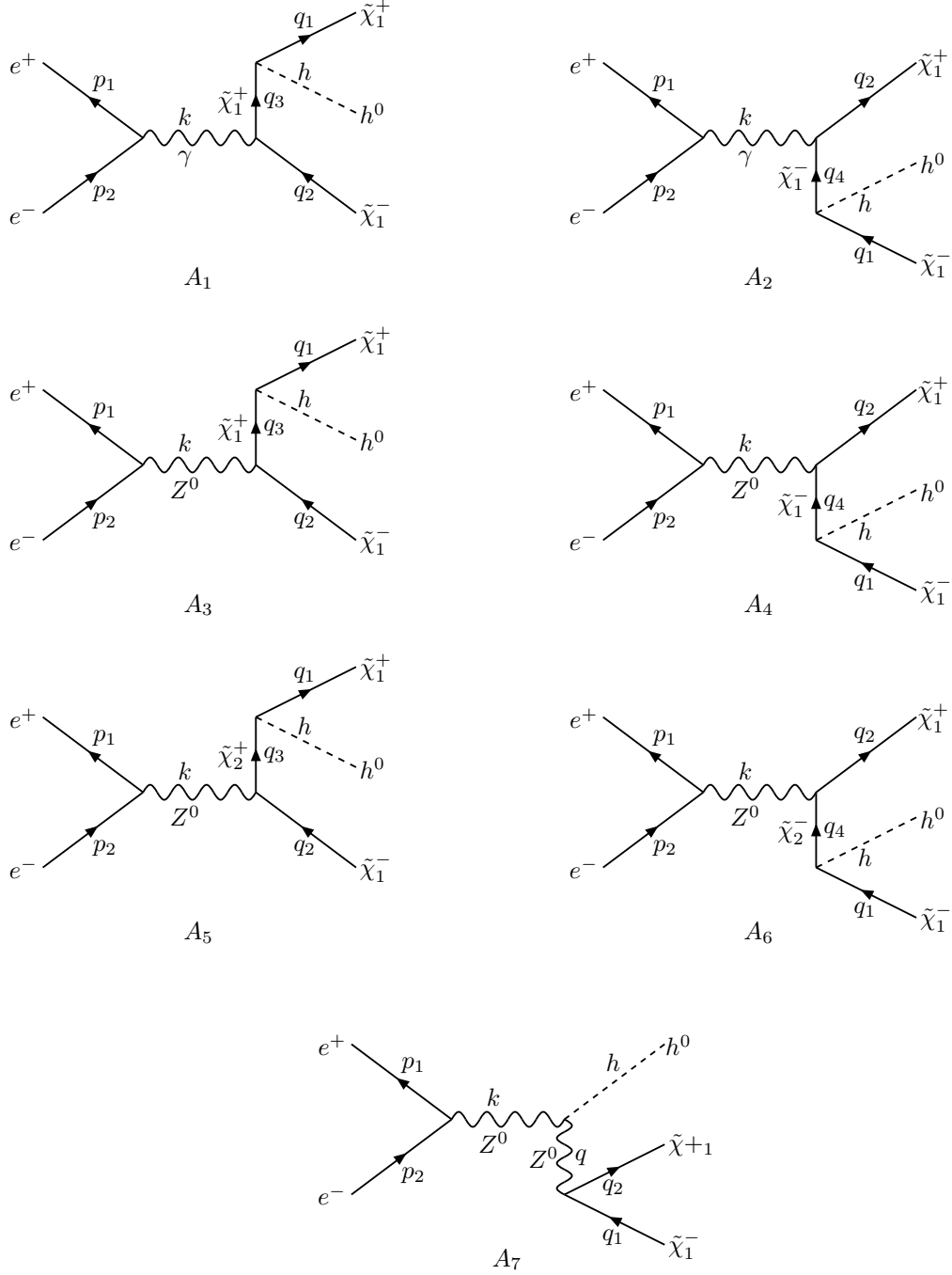


Figure 1: Set of Feynman diagrams included in the analytic Higgs-boson distribution.

while the dashed lines refer to the experimental limit on the light chargino mass ($m_{\tilde{\chi}_1^+} \simeq 100$ GeV).

The straight dot-dashed lines limit from above the region that allows the associated production of a light chargino $\tilde{\chi}_1^+$ and a resonant heavier chargino $\tilde{\chi}_2^-$ (that we are not interested in), and correspond to :

$$\sqrt{s} = m_{\tilde{\chi}_1^+} + m_{\tilde{\chi}_2^-}. \quad (3)$$

A further region of interest (beyond the grey one) could be the one where, although $\sqrt{s} > m_{\tilde{\chi}_1^+} + m_{\tilde{\chi}_2^-}$, the heavier chargino is *below* the threshold for a direct decay $\tilde{\chi}_2^+ \rightarrow \tilde{\chi}_1^+ h$. Then, again a resonant $\tilde{\chi}_2^+$ would not be allowed. The area where $m_{\tilde{\chi}_2^+} < m_{\tilde{\chi}_1^+} + m_h$ is the one inside the oblique stripes in Fig. 3. The intersection of these stripes with the area between the solid and dashed curves is a further (although quite restricted) region relevant to the non

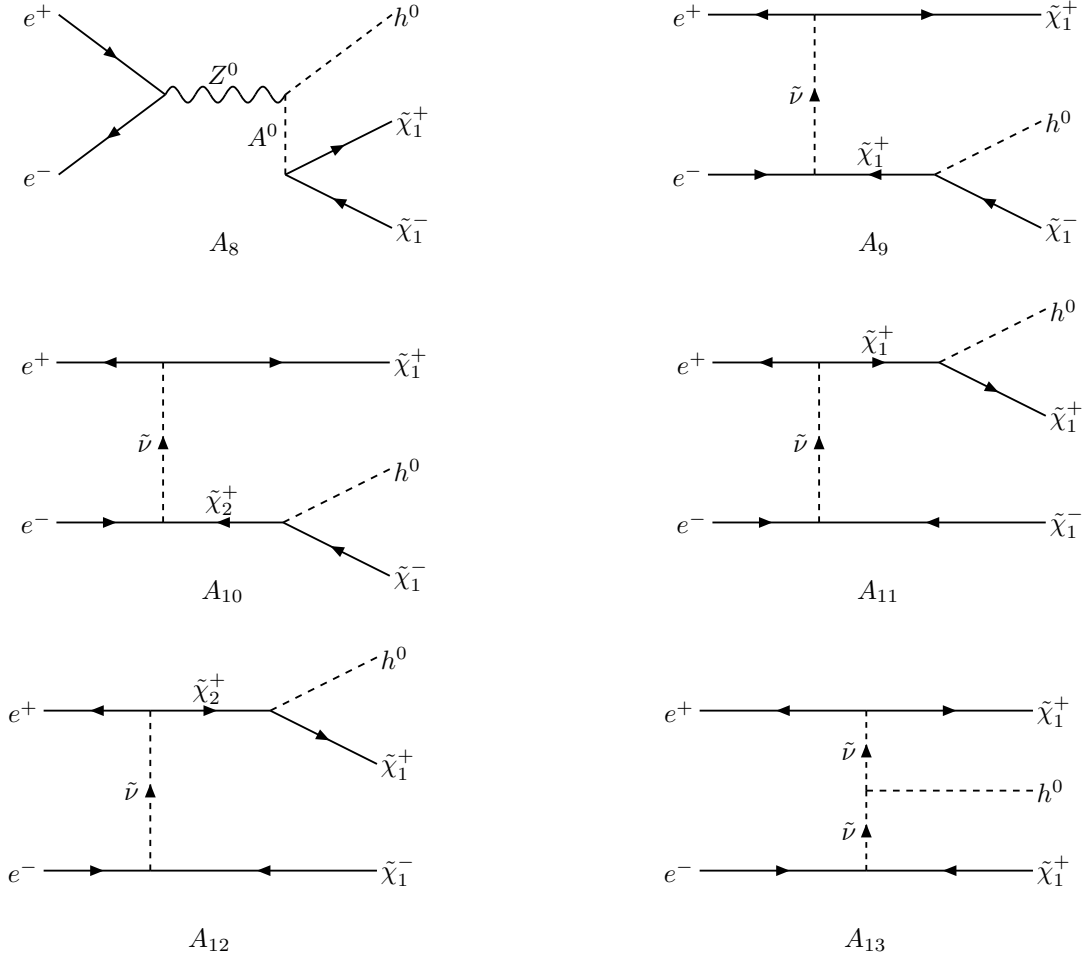


Figure 2: Set of Feynman diagrams not included in the analytic Higgs-boson distribution.

resonant $e^+e^- \rightarrow h \tilde{\chi}_1^+ \tilde{\chi}_1^-$ process. In our analysis, we did not include this parameter region, since this would have required some further dedicated elaboration of the analytic form for the $e^+e^- \rightarrow h \tilde{\chi}_1^+ \tilde{\chi}_1^-$ distributions.

3 Cross Sections and Distributions

As anticipated, our analysis concentrates on the set of 7 Feynman diagrams presented in Fig. 1. Our evaluation will then be particularly suitable in case of heavy electron sneutrinos.

The matrix elements corresponding to the amplitudes A_1, \dots, A_7 in Fig. 1 are :

$$\begin{aligned}
\mathcal{M}_1 &= \frac{ig e^2}{k^2 + i\epsilon} \bar{u}_{s_1}^\chi(q_1) (C_{11}^L P_L + C_{11}^R P_R) \frac{(\not{q}_3 + M_1)}{q_3^2 - M_1^2 + i\epsilon} \gamma^\mu v_{s_2}^\chi(q_2) \bar{v}_{r_1}^e(p_1) \gamma_\mu u_{r_2}^e(p_2) \\
\mathcal{M}_2 &= \frac{ig e^2}{k^2 + i\epsilon} \bar{u}_{s_1}^\chi(q_1) \gamma^\mu \frac{(-\not{q}_4 + M_1)}{q_4^2 - M_1^2 + i\epsilon} (C_{11}^L P_L + C_{11}^R P_R) v_{s_2}^\chi(q_2) \bar{v}_{r_1}^e(p_1) \gamma_\mu u_{r_2}^e(p_2) \\
\mathcal{M}_3 &= \frac{-ig^3}{4 \cos^2 \theta_w (k^2 - M_Z^2 + i\epsilon)} \bar{u}_{s_1}^\chi(q_1) (C_{11}^L P_L + C_{11}^R P_R) \frac{(\not{q}_3 + M_1)}{q_3^2 - M_1^2 + i\epsilon} \gamma^\mu \\
&\quad \times (O_{11}^L P_L + O_{11}^R P_R) v_{s_2}^\chi(q_2) \left(g_{\mu\nu} - \frac{k_\mu k_\nu}{M_Z^2} \right) \bar{v}_{r_1}^e(p_1) \gamma^\nu (g_V - \gamma_5) u_{r_2}^e(p_2) \\
\mathcal{M}_4 &= \frac{-ig^3}{4 \cos^2 \theta_w (k^2 - M_Z^2 + i\epsilon)} \bar{u}_{s_1}^\chi(q_1) \gamma^\mu (O_{11}^L P_L + O_{11}^R P_R) \frac{(-\not{q}_4 + M_1)}{q_4^2 - M_1^2 + i\epsilon}
\end{aligned}$$

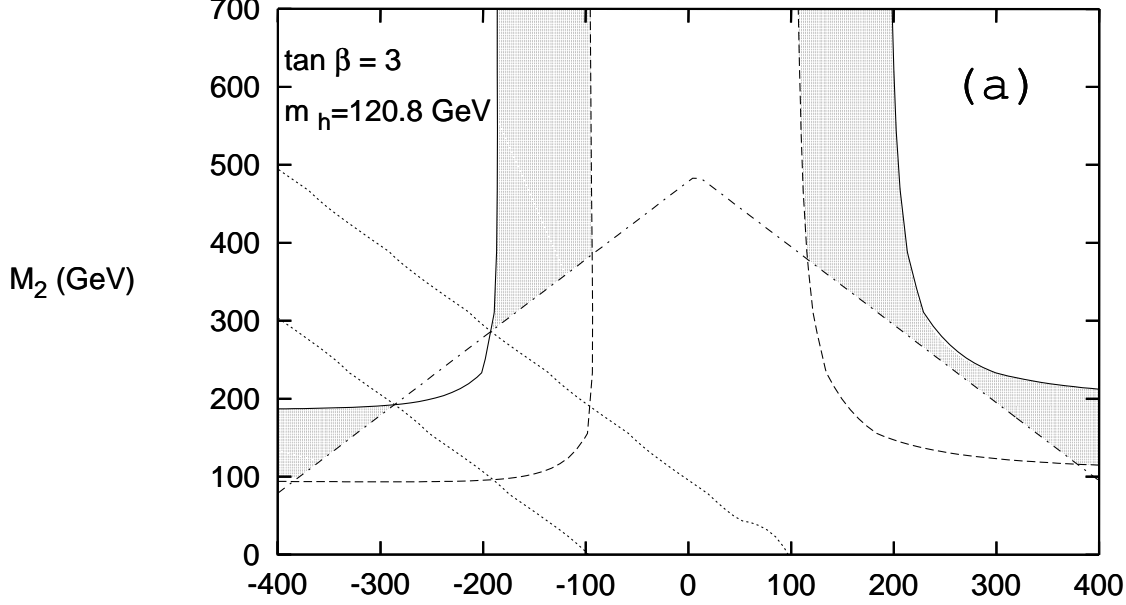


Figure 3: Parameter regions allowed for the continuum production $e^+e^- \rightarrow h \tilde{\chi}_1^+ \tilde{\chi}_1^-$ at $\sqrt{s} = 500 \text{ GeV}$, for $\tan \beta = 3$ and $M_{A^0} = 500 \text{ GeV}$ (in grey).

$$\begin{aligned}
& \times (C_{11}^L P_L + C_{11}^R P_R) v_{s_2}^\chi(q_2) \left(g_{\mu\nu} - \frac{k_\mu k_\nu}{M_Z^2} \right) \bar{v}_{r_1}^e(p_1) \gamma^\nu (g_V - \gamma_5) u_{r_2}^e(p_2) \\
\mathcal{M}_5 &= \frac{-ig^3}{4 \cos^2 \theta_w (k^2 - M_Z^2 + i\epsilon)} \bar{u}_{s_1}^\chi(q_1) (C_{12}^L P_L + C_{12}^R P_R) \frac{(\not{q}_3 + M_2)}{q_3^2 - M_2^2 + i\epsilon} \gamma^\mu \\
& \times (O_{21}^L P_L + O_{21}^R P_R) v_{s_2}^\chi(q_2) \left(g_{\mu\nu} - \frac{k_\mu k_\nu}{M_Z^2} \right) \bar{v}_{r_1}^e(p_1) \gamma^\nu (g_V - \gamma_5) u_{r_2}^e(p_2) \\
\mathcal{M}_6 &= \frac{-ig^3}{4 \cos^2 \theta_w (k^2 - M_Z^2 + i\epsilon)} \bar{u}_{s_1}^\chi(q_1) \gamma^\mu (O_{12}^L P_L + O_{12}^R P_R) \frac{(-\not{q}_4 + M_2)}{q_4^2 - M_2^2 + i\epsilon} \\
& \times (C_{21}^L P_L + C_{21}^R P_R) v_{s_2}^\chi(q_2) \left(g_{\mu\nu} - \frac{k_\mu k_\nu}{M_Z^2} \right) \bar{v}_{r_1}^e(p_1) \gamma^\nu (g_V - \gamma_5) u_{r_2}^e(p_2) \\
\mathcal{M}_7 &= \frac{ig^3 M_Z \sin(\beta - \alpha)}{4 \cos^3 \theta_w} \bar{u}_{s_1}^\chi(q_1) \gamma^\mu (O_{11}^L P_L + O_{11}^R P_R) v_{s_2}^\chi(q_2) \\
& \times \frac{(g_{\mu\nu} - q_\mu q_\nu / M_Z^2)}{(q^2 - M_Z^2 + i\epsilon)} \frac{(g^{\nu\sigma} - k^\nu k^\sigma / M_Z^2)}{(k^2 - M_Z^2 + i\epsilon)} \bar{v}_{r_1}^e(p_1) \gamma_\sigma (g_V - \gamma_5) u_{r_2}^e(p_2), \tag{4}
\end{aligned}$$

where

$$k = p_1 + p_2 = q_1 + q_2 + h, \quad q_3 = q_1 + h, \quad q_4 = q_2 + h, \quad q = p_1 + p_2 - h,$$

and $M_{1,2} = m_{\tilde{\chi}_{1,2}^\pm}$.

All external momenta are defined in Fig. 1, as flowing from the left to the right, and different couplings in Eq. (4) are defined in [1]. The lower indices of the spinors u, v refer to the particle spin.

We squared, averaged over the initial spin, and summed over the final spin the sum of the matrix elements in Eq. (4)

with the help of FORM [14]. Then, we performed a double analytic integration over the phase-space variables. This allowed us to obtain an exact *analytic* expression for the Higgs-boson momentum distribution

$$E_h \frac{d\sigma}{d^3\mathbf{h}} = \frac{\beta}{s(4\pi)^5} \int_{-1}^1 d\cos\vartheta \int_0^{2\pi} d\varphi |\overline{\mathcal{M}}|^2 = f(p_1, p_2, h), \quad (5)$$

where $\mathcal{M} = \sum_{i=1}^7 \mathcal{M}_i$. The complete code, including the analytic result for $E_h \frac{d\sigma}{d^3\mathbf{h}}$ (that is a quite lengthy expression), and the numerical integration routine that allows a fast evaluation of the total cross section, is available from the authors' e-mail addresses.

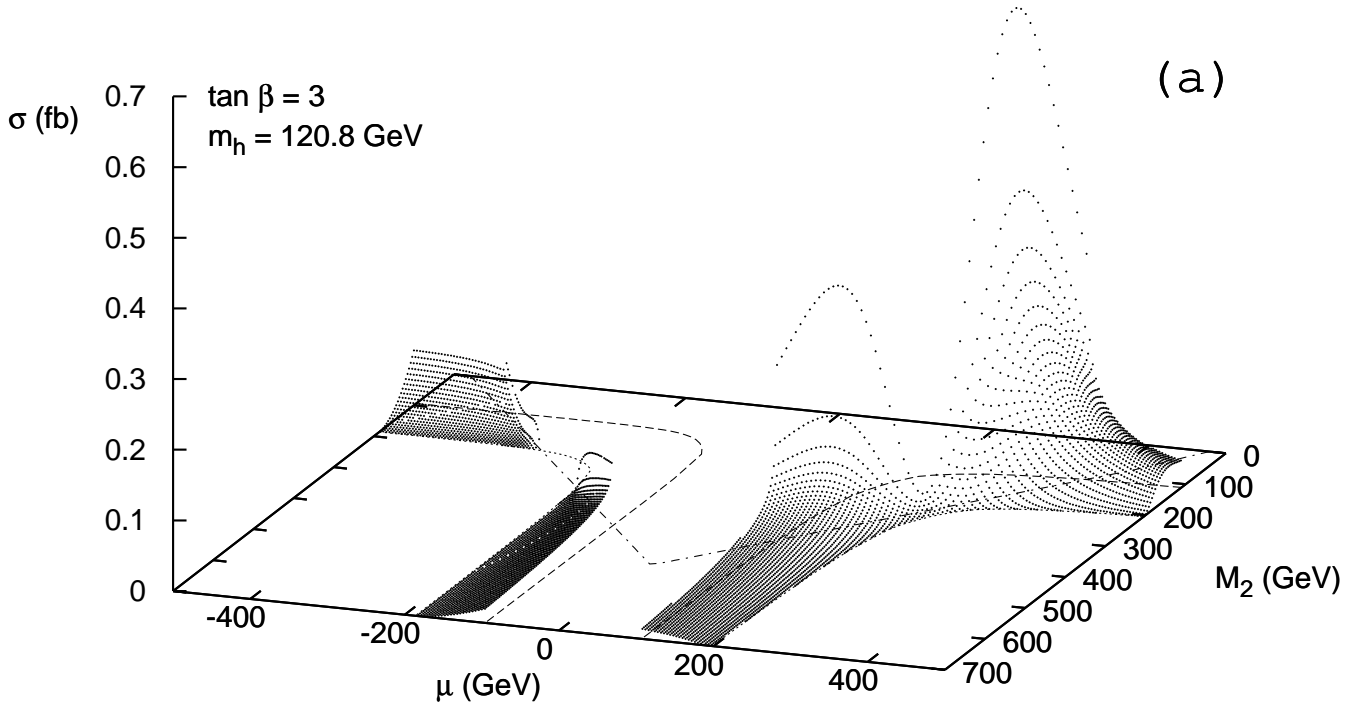


Figure 4: Total cross section for $e^+e^- \rightarrow h \tilde{\chi}_1^+ \tilde{\chi}_1^-$ at $\sqrt{s} = 500 \text{ GeV}$, for $\tan \beta = 3$ and $M_{A^0} = 500 \text{ GeV}$.

In Fig. 4, we show the total cross section for $e^+e^- \rightarrow h \tilde{\chi}_1^+ \tilde{\chi}_1^-$ at $\sqrt{s} = 500 \text{ GeV}$. We obtained it by numerically integrating over the Higgs-boson energy and angle the analytic distribution in Eq. (5). In Fig. 4, we scan the relevant (μ, M_2) parameter space for $|\mu| < 500 \text{ GeV}$, and $M_2 < 700 \text{ GeV}$. Cross sections of a few 0.1 fb^{-1} are reached in a good portion of the allowed regions especially for positive μ . We checked that our results completely agree with the cross section evaluated by CompHEP [15] on the basis of the same set of Feynman diagrams of Fig. 1.

We studied quantitatively the consequence of disregarding the 6 diagrams in Fig. 2, involving either pseudoscalar or sneutrino exchange, by comparing our results with the cross section corresponding to the complete set of 13 diagrams, computed by CompHEP. While the pseudoscalar-exchange diagram never contributes sizable for $m_{A^0} = 500 \text{ GeV}$, the influence of the 5 sneutrino-exchange diagrams depends critically on $m_{\tilde{\nu}_e}$ and also on the relative importance of the gaugino-higgsino components in the chargino [1].

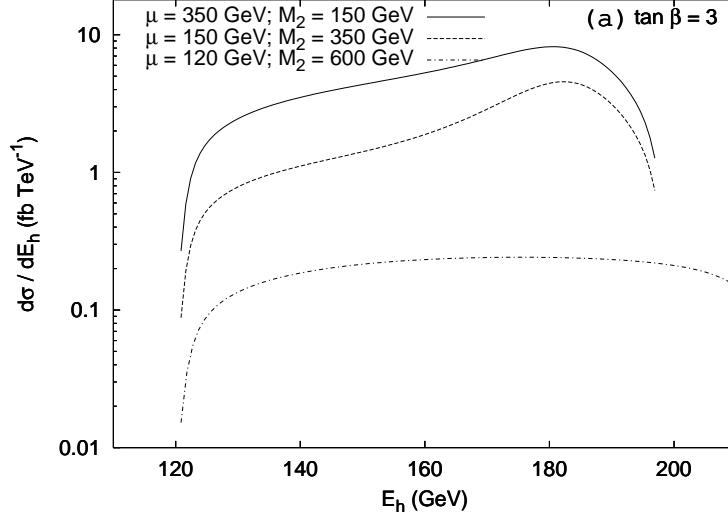


Figure 5: Higgs-boson energy distribution in the e^+e^- c.m. frame in $e^+e^- \rightarrow h \tilde{\chi}_1^+ \tilde{\chi}_1^-$ at $\sqrt{s} = 500 \text{ GeV}$, for $\tan \beta = 3$, $M_{A^0} = 500 \text{ GeV}$.

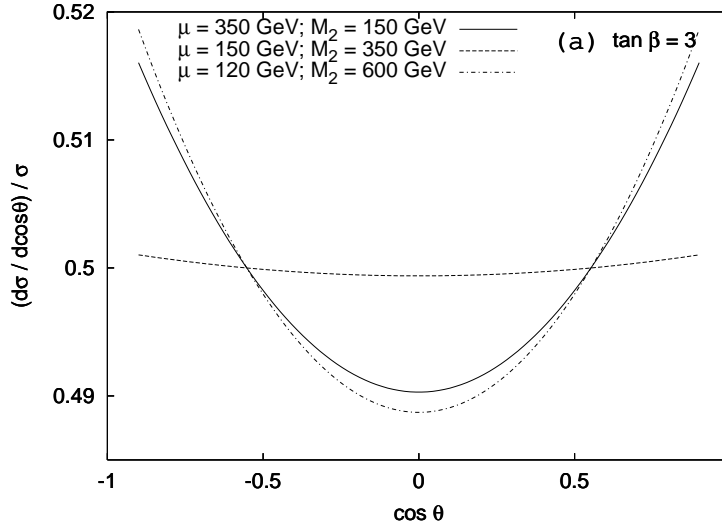


Figure 6: Higgs-boson angular distribution in the e^+e^- c.m. frame in $e^+e^- \rightarrow h \tilde{\chi}_1^+ \tilde{\chi}_1^-$ at $\sqrt{s} = 500 \text{ GeV}$, for $\tan \beta = 3$, $M_{A^0} = 500 \text{ GeV}$.

We also considered the $e^+e^- \rightarrow h \tilde{\chi}_1^+ \tilde{\chi}_1^-$ cross sections at the higher-energy extension expected for a linear-collider project [2]. Going at $\sqrt{s} \simeq 1 \text{ TeV}$, our treatment of the $e^+e^- \rightarrow h \tilde{\chi}_1^+ \tilde{\chi}_1^-$ cross section becomes less accurate. As far as production rates are concerned, for chargino and Higgs-boson masses not much heavier than present experimental limits, and heavy sneutrinos, the $\sqrt{s} = 500 \text{ GeV}$ phase of the linear collider could be the best option to study the process $e^+e^- \rightarrow h \tilde{\chi}_1^+ \tilde{\chi}_1^-$.

We finally studied the behavior of Higgs-boson energy and angular distributions versus the MSSM parameters. In Figs. 5 and 6, we plot energy and angular distributions in the e^+e^- c.m. frame, as obtained by numerically integrating over one variable Eq. (5). Both the energy- and angular-distribution shapes are considerably influenced by the gaugino/higgsino composition of the light chargino, and by a possible saturation of the available phase-space [1].

4 Conclusions

We analyzed the associated production of a light Higgs boson and a light-chargino pair in the MSSM at $\sqrt{s} = 500 \text{ GeV}$ e^+e^+ linear colliders. The process was discussed in the region of the MSSM parameter space where there is no resonant production of either the heavier chargino or the pseudoscalar Higgs boson A and in the limit of heavy sneutrino masses ($m_{\tilde{\nu}_e} > 1 \text{ TeV}$). We computed analytically distributions in the Higgs-boson momentum. We obtained cross sections up to a few 0.1 fb (for $\mu > 0$) for masses not much heavier than present experimental limits. These rates make this process potentially detectable at $\sqrt{s} = 500 \text{ GeV}$ e^+e^- LC with an integrated luminosity of the order of 1000 fb^{-1} . This could allow a first determination of the $h \tilde{\chi}_1^+ \tilde{\chi}_1^-$ production rate with a statistical error of the order of 10%, that, in absence of further systematics, could be extrapolated to a determination of the $h \tilde{\chi}_1^+ \tilde{\chi}_1^-$ coupling with comparable accuracy. Future studies in this direction are required for a more solid assessment of the potential of this process.

References

- [1] G. Ferrera and B. Mele, arXiv:hep-ph/0406256.
- [2] E. Accomando *et al.* [ECFA/DESY LC Physics Working Group Collaboration], Phys. Rept. **299** (1998) 1. [arXiv:hep-ph/9705442];
J. A. Aguilar-Saavedra *et al.* [ECFA/DESY LC Physics Working Group Collaboration], arXiv:hep-ph/0106315;
K. Abe *et al.* [ACFA Linear Collider Working Group Collaboration], arXiv:hep-ph/0109166;
T. Abe *et al.* [American Linear Collider Working Group Collaboration], in *Proc. of the APS/DPF/DPB Summer Study on the Future of Particle Physics (Snowmass 2001)* ed. N. Graf, arXiv:hep-ex/0106055 ; arXiv:hep-ex/0106056 ; arXiv:hep-ex/0106057 ; arXiv:hep-ex/0106058.
- [3] K. J. Gaemers and G. J. Gounaris, Phys. Lett. B **77** (1978) 379;
A. Djouadi, J. Kalinowski and P. M. Zerwas, Mod. Phys. Lett. A **7** (1992) 1765 and Z. Phys. C **54** (1992) 255;
J. F. Gunion, B. Grzadkowski and X. G. He, Phys. Rev. Lett. **77** (1996) 5172, [arXiv:hep-ph/9605326] ;
H. Baer, S. Dawson and L. Reina, Phys. Rev. D **61** (2000) 013002, [arXiv:hep-ph/9906419] ;
A. Juste and G. Merino, arXiv:hep-ph/9910301 ;
S. Moretti, Phys. Lett. B **452** (1999) 338, [arXiv:hep-ph/9902214] ;
A. Denner, S. Dittmaier, M. Roth and M. M. Weber, arXiv:hep-ph/0309274 and references therein.
- [4] G. Belanger, F. Boudjema, T. Kon and V. Lafage, Eur. Phys. J. C **9** (1999) 511, [arXiv:hep-ph/9811334] ;
A. Djouadi, J. L. Kneur and G. Moultaka, Nucl. Phys. B **569** (2000) 53, [arXiv:hep-ph/9903218].
- [5] A. Djouadi, J. L. Kneur and G. Moultaka, Phys. Rev. Lett. **80** (1998) 1830, [arXiv:hep-ph/9711244]. A. Dedes and S. Moretti, Phys. Rev. D **60** (1999) 015007 [arXiv:hep-ph/9812328] and Eur. Phys. J. C **10** (1999) 515. [arXiv:hep-ph/9904491] ;
G. Belanger, F. Boudjema and K. Sridhar, Nucl. Phys. B **568** (2000) 3, [arXiv:hep-ph/9904348].
- [6] A. Datta, A. Djouadi and J. L. Kneur, Phys. Lett. B **509** (2001) 299 [arXiv:hep-ph/0101353].
- [7] A. Brignole, G. Degrassi, P. Slavich and F. Zwirner, Nucl. Phys. B **631** (2002) 195 [arXiv:hep-ph/0112177] and Nucl. Phys. B **643** (2002) 79 [arXiv:hep-ph/0206101].
- [8] LEPSUSYWG, ALEPH, DELPHI, L3 and OPAL experiments, note LEPSUSYWG/01-03.1 and note LEPSUSYWG/02-04.1 (<http://lepsusy.web.cern.ch/lepsusy/Welcome.html>).
- [9] M. Baillargeon, F. Boudjema, F. Cuypers, E. Gabrielli and B. Mele, Nucl. Phys. B **424** (1994) 343 [arXiv:hep-ph/9307225].
- [10] H. E. Haber and G. L. Kane, Phys. Rept. **117** (1985) 75 .
- [11] ALEPH, DELPHI, L3, OPAL Collaborations and the LEP Higgs Working Group, LHWG Note 2001-4 [ALEPH 2001-057, DELPHI 2001-114, L3 Note 2007, OPAL Technical Note TN699], CERN preprint 2001; OPAL Collaboration, OPAL PN524, CERN preprint 2003.
- [12] R. Barate *et al.* [ALEPH, DELPHI, L3, OPAL Collaborations and LEP Working Group for Higgs boson searches], Phys. Lett. B **565** (2003) 61 [arXiv:hep-ex/0306033].
- [13] S. Heinemeyer, W. Hollik and G. Weiglein, “FeynHiggsFast: A program for a fast calculation of masses and mixing angles in the Higgs sector of the MSSM”, arXiv:hep-ph/0002213.
- [14] J.A.M. Vermaseren, *Symbolic Manipulation with FORM*, published by CAN (Computer Algebra Nederland), Kruislaan 413, 1098 SJ Amsterdam, 1991, ISBN 90-74116-01-9.
- [15] A. Pukhov *et al.*, “CompHEP: A package for evaluation of Feynman diagrams and integration over multi-particle phase space. User’s manual for version 33”, arXiv:hep-ph/9908288;
A. Semenov, “CompHEP/SUSY package”, Nucl. Instrum. Meth. A **502** (2003) 558 [arXiv:hep-ph/0205020].